Geophysical Research Letters

RESEARCH LETTER
10.1029/2021GL093622

Natural Variability and Warming Signals in Global Ocean Wave Climates

I. Odériz[1], R. Silva[1], T.R. Mortlock[2,3], N. Mori[4], T. Shimura[4], A. Webb[4], R. Padilla-Hernández[5], and S. Villers[6]

[1]Instituto de Ingeniería, Universidad Nacional Autónoma de México, México, [2]Risk Frontiers, Australia, [3]Department of Earth and Environmental Sciences, Macquarie University, Australia, [4]Disaster Prevention Research Institute, Kyoto University, Japan, [5]IMSG at National Oceanic and Atmospheric Administration NOAA, MD, USA, [6]Facultad de Ciencias, Universidad Nacional Autónoma de México, México

Key Points:

- The global ocean wave climate is classified into types according to the planetary wind systems responsible for their genesis
- In general, natural variability is shown to be the principal signal in wave climate types over the past 34 years
- Signals showing global warming have already emerged in the Indian Ocean, and the tropical regions of the Atlantic and Pacific Oceans

Supporting Information:

Supporting Information may be found in the online version of this article.

Correspondence to:

I. Odériz,
itxaso.oderiz@gmail.com

Citation:

Odériz, I., Silva, R., Mortlock, T. R., Mori, N., Shimura, T., et al. (2021). Natural variability and warming signals in global ocean wave climates. *Geophysical Research Letters*, *48*, e2021GL093622. https://doi.org/10.1029/2021GL093622

Received 31 MAR 2021
Accepted 10 MAY 2021

Abstract This paper presents a multivariate classification of the global wave climate into types driven by atmospheric circulation patterns. The primary source of the net long-term variability is evaluated based on historical wave simulations. Results show that the monsoon, extratropical, subtropical, and polar wave climate types of the Pacific and North Atlantic Oceans are dominated by natural variability, whereas the extratropical and subtropical wave climate types in the Indian Ocean, and the tropical wave climate types of the Atlantic and Pacific Oceans exhibit a global warming signal. In the Pacific sector of the Southern Ocean, strong natural variability may mask a global warming signal that is yet to emerge as being statistically significant. In addition, wave climate teleconnections were found across the world that can provide a framework for joint strategies to achieve the goals of climate adaption for resilient coastal communities and environments.

Plain Language Summary Near-surface wind systems drive global ocean wave conditions that are usually studied at regional or local scale. However, analyzing these relationships at the global scale is important to understand how natural climate oscillations, such as El Niño-Southern Oscillation, and global warming, impact wave climate. Here we identify the large wave climates in homology to the climate regions (e.g., Tropical, Temperate, Polar) and are originated by the planetary wind systems. The results show that global warming signals have already emerged in the Indian Ocean and the tropical regions of the Pacific and Atlantic basins. In contrast, in the other ocean basins, natural variability is still the dominant signal and could mask global warming signals.

1. Introduction

Long-term variations of wave climate affect a wide range of activities and processes in which wave hydrodynamics play an essential role, such as port operability (Izaguirre et al., 2020), wave energy resources (Fairley et al., 2020), marine and coastal ecosystems (Fraser et al., 2018; Odériz, Gómez, et al., 2020), and water quality (Erftemeijer et al., 2012; Huizer et al., 2019). Furthermore, changes in wave run-up may significantly increase the risk of coastal erosion (Luijendijk et al., 2018; Ranasinghe, 2016; Toimil et al., 2020) and flooding (Kirezci et al., 2020; Melet et al., 2018). Over the longer-term, shifts in the power and directionality of wave climate can impact sediment transport patterns and large scale coastal morphology. Therefore, deciphering the relative importance of natural variability and global warming is a key starting point to rebuild coastal environments (UN-SDG 14) and adapting to climate change (COP21-Paris).

Under climate warming scenarios, wave climate is projected to shift clockwise in most of the world´s oceans, and intensify in the Southern Ocean (Hemer, Katzfey, et al., 2013; Morim et al., 2019; Reguero et al., 2019; Ribal & Young, 2019) South Atlantic, and Indian Oceans (Lobeto et al., 2021; Meucci et al., 2020). Superimposed on this, natural variability strongly influences wave climate characteristics (Hemer et al., 2010; Odériz, Silva, Mortlock, & Mori, 2020) from interannual to multidecadal timescales. This is forced by climate patterns, such as the El Niño-Southern Oscillation (ENSO) or the Southern Annular Mode (SAM). For instance, in 2015, an extreme El Niño event caused large swells across the South and East Pacific, leading to many casualties and severe economic losses in Latin America (Godwyn-Paulson et al., 2020).

The delineation between the roles of long-term variability and global warming in wave climate is an important, yet under-studied, area of ocean wave science. First, natural variability can mask a global warming signal in areas with a high level of natural fluctuation (Clem et al., 2020; Tebaldi et al., 2011). Second, natural variability can delay the restoration and adaptability to climate change of natural and human systems (Duarte et al., 2020; Moser & Ekstrom, 2010). And finally, natural variability can dampen or amplify the hazards associated with global warming (Deser et al., 2012). For these reasons, understanding the extent to which changes in wave climate are presently driven by global warming, natural variability, or both, is pivotal to sustainable coastal management.

This study aims to classify the global ocean wave climate into types that are linked to the atmospheric circulation responsible for their genesis. We evaluate the impact of each source, natural variability and global warming, in the net long-term variation and trends of each wave climate type over the last three decades. Moreover, we elucidate ocean-wave teleconnection patterns that connect the world's coasts, having a similar wave climate response to the atmospheric circulation. We propose a novel "dynamic clustering" approach to identify the major wave climates, defined as areas having similar prevailing wave conditions, in homology to the major climate regions (e.g., tropical, temperate). Although we are not examining extreme events, this wave climate framework is crucial for addressing effective coastal hazard and planning strategies as results pertain to long-term shifts in the bulk wave climate. We propose that these results can also be used to: a) prioritize coastal areas where the effects of global warming has already emerged, and those where natural variability still dominates; and b) as a basis for defining large-scale coastal assessment based on wave climate regions, that may experience similar changes through time.

2. A General Perspective of the Methods

This section presents a summary of the methods applied for wave climate classification, natural variability, long-term trends, and teleconnection detection. For more details of these methods see Supplementary Information, Text S1, Figure S1–S5, Table S1–S2. The ocean wave and wind monthly averaged parameters of the ERA-5 (Hersbach et al., 2020) data-set for 1979–2018 were used in this study.

We apply a "dynamic clustering" methodology based on the *k-means* (MacQueen, 1967) technique to examine the planetary wind systems using surface wind velocity ($U_{10,}$ m/s) and wind direction ($Dir_{w,}$ º). The direction is decomposed into sine and cosine components, and the variables ($U_{10,}$ $cos(Dir_w)$, $sin(Dir_w)$) are normalized. All the time-steps and space-grid values of a parameter is a unique variable. That means, the 3D matrix (longitude, latitude, time) of each parameter (i.e., (U_{10}, $cos(Dir_w)$, $sin(Dir_w)$ is reshaped to a 1D array, and once *k-means* is applied, the classification is reshaped back from a 1D array to a 3D matrix, see Supplementary Figure S2 and Equation S2. The optimal number of clusters were selected using the Elbow Method (Ketchen & Shook, 1996). The resultant classification identifies the spatial-temporal distribution of the wind systems and provides a set of indices to identify the atmospheric circulation and its variability.

Next, the wave climates, defined as the regions in the global oceans with similar wave direction and power, are calculated using the same "dynamic clustering" approach, but this time the input variables are the wave direction ($Dir_{m,}$ º) and wave power (P_w, kW/m). The mean wave direction is a critical component of coastal sediment transport (Barnard et al., 2015; Hemer et al., 2010). While wave power is the wave energy flux and is a key parameter for coastline stability (Ranasinghe, 2016), coastal structures, and wave energy extraction (Reguero et al., 2015). Furthermore, previous studies have shown that global wave power and sea surface temperature (SST) are strongly linked (Shimura et al., 2020) and P_w may be a good indicator of the global warming signal inherent in wave climate (Reguero et al., 2019). The process resulted in three major global wave climates that are: the westerlies, easterlies and southerlies.

The three wave climates are further decomposed into Wave Climate Types (WCTs) that are independent wave climates generated by basin-scale wind systems, propagating outwards from the generation area. These were obtained by identifying the isolated areas of the major global wave climates and relating them with their basin-scale wind origin. If the spatial area and directional range of a WCT is shared by a wind system, then that WCT is generated by the paired wind system. If the WCT has no obvious wind system pairing, the origin of the WCT is considered as swell with an undefined wind system origin.

Once the WCTs were obtained, the time series of the total occupied area, $A_{T,t}$, and the spatial mean wave direction and wave power, $Dir_{m,t}, Pw_{m,t}$, were calculated. The natural variability of these parameters were analyzed by de-trending and computing the composite monthly anomalies of the periods of ENSO, ENSO-PDO (Pacific Decadal Oscillation), and ENSO-SAM coupling, over the satellite era (1985–2018) (Ribal & Young, 2019), and only those that were statistically significant were considered. ENSO phases were identified using the Oceanic Niño Index, and PDO with the PDO index of NOAA. The SAM phases were calculated using the monthly Antarctic Oscillation index (where positive SAM > μ+σ; and negative SAM < μ−σ), following the indications of (Godoi & Júnior, 2020; Marshall et al., 2018).

The long-term trends of the spatially averaged P_w and Dir_m of WCTs were calculated using the Least Squares approach, for the same period as the natural variability analysis (1985–2018). The Mann-Kendall (Hirsch et al., 1982) approach was used, at the 95% confidence level, to calculate the significance of the trends. In order to address the underlying mechanisms responsible for these trends, we also calculated trends for the spatially averaged velocity of surface winds (U_{10}) systems and SSTs for the identical areas occupied by each WCT over the same time period. We assume that any long-term trends in wave power and direction of WCTs that is concurrent with trends in SSTs or surface winds in the same climate region have a causal relationship.

Finally, the total area, A_t, and spatial-averages of Dir_m, and P_{wm} of each WCT were correlated with those of every other WCT to quantify their interconnection, using the Pearson correlation coefficient (Kendall, 1948) with a level of confidence of 95%.

2.1. Ocean Wave Climate Types Driven by Atmospheric Circulation

We identify a global set of major wave climates (Figure 1) that have the same spatial-temporal patterns as the planetary wind systems (Figure S6) that drive them, and a subset of seven WCTs implicitly linked to the basin-scale wind systems responsible for their generation. The westerly wave climate is defined as a high-energy system (the averaged wave power in the cluster is ~59 kW/m) with wave directions from 209°–352°, which encompass the extratropical, monsoon, and warm pool WCTs. The southerly wave climate is defined as a moderate-energy system (the averaged wave power in the cluster ~27 kW/m), which travels in a northward direction (between 135° and 216°), and includes the subtropical and subpolar WCTs. The easterly wave climate is defined as a low-energy system (the averaged wave power in the cluster ~18 kW/m), with directions between 6° and 138°, and includes the tropical and polar WCTs. All the wave climates identified in this study are swell-dominated, in agreement with (Li, 2016; Semedo et al., 2011). This is particularly true for the easterly and southerly wave climates (see Figure S7 and S8).

The wind sea wave power and wind velocity pertaining to each WCT were correlated. A high correlation (R > 0.7) was found for all WCTs, and a very high correlation for the easterlies and westerlies (R > 0.9). The covariance was also computed, using standardized values (Figure S7). This confirms that the majority of the variability in the WCTs is driven by the planetary wind systems, which in turn are the result of pressure gradients between High and Low pressure atmospheric systems. From this, the variability in the polar and extratropical WCTs of the North Pacific and North Atlantic is related to the strength and position of the Aleutian Low and the Icelandic Low. Variations in all tropical WCTs are related to the trade winds, and as such their intensification is influenced by the northern Hadley cell in the Atlantic and Pacific, and the southern Hadley cell in the Indian Ocean. The subtropical WCTs are controlled by the position and strength of the subtropical ridges, whereas the subpolar WCTs are linked to the subpolar ridges. The relationship between sea level pressure, wind, and WCTs, and their seasonal variability, is fully explained in Supplementary Information Text S3 and Figure S7–S18.

The link between planetary winds, pressures systems, and WCTs, gives us a fuller understanding of the causal mechanisms between the climate patterns, global warming and wave climate, and provides a more accurate quantification of their impacts. Moreover, the findings regarding these WCTs are in agreement with previous studies on global wave variability (Echevarria et al., 2020; Hemer, Fan, et al., 2013; Reguero et al., 2019; Shimura et al., 2013; Stopa & Cheung, 2014) and swell wave generation (Alves, 2006; Li, 2016;

Wave Climates	Wave Climates Types (WCTs)	Ocean Basin
Easterlies	Polar	North Atlantic, North Pacific Oceans
	Tropical	Atlantic, Pacific, Indian Oceans
Southerlies	Subtropical	South Pacific, North Pacific, North Atlantic, South Atlantic,Indian Oceans
	Subpolar	North Atlantic, North Pacific Oceans
Westerlies	Extratropical	South Pacific, North Pacific, North Atlantic, South Atlantic, and Indian Oceans
	Monsoon	Indian Ocean
	Warm Pool	Indian and Pacific Oceans

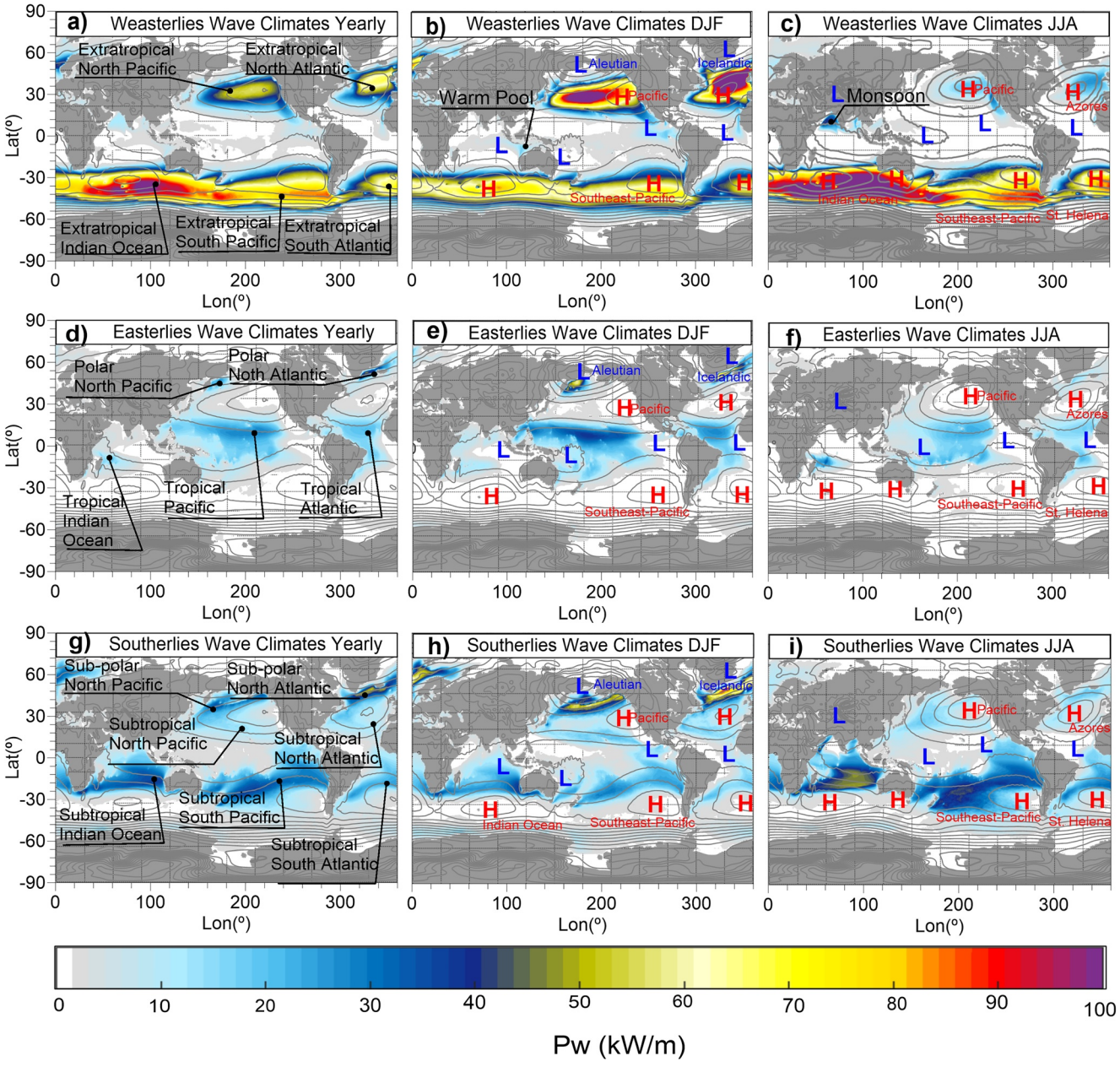

Figure 1. Global wave climates classified by dynamic clustering. P_w (kW/m), yearly averaged (a, d, g), DJF (b, e, h), and JJA (c, f, i), of the westerlies (a, b, c), easterlies (d, e, f), and southerlies (g, h, i) wave climates. Gray contour lines indicate the average sea level pressure (SLP). H and L indicate the high and low-pressure centers of the SLP.

a)

Wave Climate	Wave Climate Type	Basin	Natural variability: Tropical and extratropical Composite anomalies P_{wm}(kW/m)										Trend Increment over 34 yrs			Global Warming Increment over 34 yrs
			ENSO +	ENSO -	ENSO + PDO +	ENSO + PDO -	ENSO + SAM +	ENSO + SAM -	ENSO - PDO +	ENSO - PDO -	ENSO - SAM +	ENSO - SAM -	P_{wm} (kW/m)	P_{wm} Wind sea (kW/m)	U_{10} (m/s)	SST (Cº)
Southerlies	Subtropical	Indian Ocean	-	0.74	-	-1.1	-	-	-	1.04	2.11	-	3.95	0.36	0.18	0.63
Southerlies	Subtropical	South Pacific	-	-	-	-	2.45	-	-	-	-	-2.11	-	-	-	-
Southerlies	Subtropical	North Pacific	-	-	-	-	-	-	-	-	-	9.98	-	-	-	-
Southerlies	Subpolar	North Pacific	-	-	-	-	-	-	-	-	-	-	-	-	-	-
Southerlies	Subtropical	South Atlantic	-	-	-	-	-	-	-	-	-	-	2.76	0.47	0.25	-
Southerlies	Subtropical	North Atlantic	-	-	-	-	-	-	-	-	-	-8.92	-	-	-	-
Southerlies	Subpolar	North Atlantic	-	-	-	-	-	-	-	-	-	-7.52	-	-2.68	-	-
Westerlies	Extratropical	Indian Ocean	-	-	2.15	-	6.8	-	-	-	5.53	-	9.03	-	0.17	0.33
Westerlies	Warm Pool	Indian Ocean	-	-	-	-1.4	-	-	-	-	2.33	-	1.59	-	-	0.68
Westerlies	Monsoon	Indian Pacific	-	0.71	-	-	-1.06	-	-	0.8	2.9	-	-	-	-	0.84
Westerlies	Extratropical	South Pacific	-1.58	2.88	-	-3.37	5.49	-9.32	-	4.5	9.67	-7.77	6.52	-	-	-
Westerlies	Extratropical	North Pacific	2.58	-	3.4	-	4.48	3.89	-	-	-	-	-	-	-	-
Westerlies	Extratropical	South Atlantic	-	-	1.54	-	4.17	-	-2.8	-	-	-	5.9	1.76	0.29	-
Westerlies	Extratropical	North Atlantic	-	-	-	-	-	-	-	-	-	-	-	-	-	-
Easterlies	Tropical	Indian Ocean	-1.14	-	-1.75	-	-	-	-	-	2.37	-	-	-	-	0.63
Easterlies	Tropical	Pacific	0.79	-	0.78	-	2.06	-	-1.24	-	-	-	2.52	0.36	0.23	0.55
Easterlies	Polar	North Pacific	-	-	-	-	-	-	-	-	-	-	-	-	-	-
Easterlies	Tropical	Atlantic	-	-	-	-	-	-	-	-	-	-	1.83	0.4	0.15	0.61
Easterlies	Polar	North Atlantic	-	-3.48	-	-	-	-	-7.67	-	-	-6.23	-	-	-	-

$\triangle P_w$(kW/h): -10, -7.5, -5, -2.5, 0, 2.5, 5, 7.5, 10

$\triangle$SST (C°): 0, 0.25, 0.5, 0.75, 1

b)

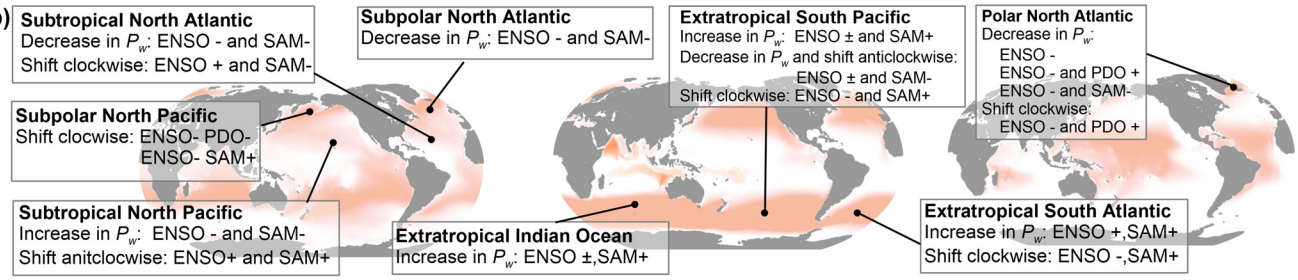

Figure 2. (a) Composite anomalies of wave power induced by tropical and extratropical climate variability, and trends of wave power, wind-sea wave power, near-surface wind velocity, and sea surface temperature, associated with each wave climate types between 1985 and 2018 (only the anomalies and trends that are significant at 95% confidence levels are shown), (b) summary of the most relevant wave climate impacts.

Semedo et al., 2011). Indeed, some of the WCTs shown here exhibit the same spatial patterns as those obtained by other authors (Echevarria et al., 2019; Jiang, 2020).

3. Tropical and Extratropical Natural Variability

The interannual variability of the global wave climate is principally governed by ENSO (Barnard et al., 2015; Odériz, Silva, Mortlock, & Mori, 2020; Stopa & Cheung, 2014). The ENSO signal can be either amplified or dampened by extratropical, multidecadal signals, such as the PDO (Newman et al., 2003) and SAM (Clem et al., 2020), that in turn impact ocean wave conditions (Bromirski et al., 2013; Godoi & Júnior, 2020; Hemer et al., 2010; Odériz, Silva, Mortlock, & Mori et al., 2020). SAM is also the dominant large-scale pattern of the Southern Ocean (Wang & Cai, 2013). To elucidate the role of tropical and extratropical variability on wave climate, we investigate the responses of the WCTs to ENSO, and ENSO coupled with the SAM and PDO. For each WCT, the composite anomalies of the spatially averaged wave power are shown in Figure 2a), with mean wave direction in Table S3.

Wave power associated with the extratropical WCTs appears to be most impacted by tropical-extratropical climate variability (ENSO, PDO and SAM). Accordingly, the results show that El Niño events strengthen the extratropical WCT in the North Pacific ($\sim +3$ kW/m), as the ENSO positive phase is associated with a strengthened Aleutian Low (Li et al., 2015). This effect is amplified when ENSO and PDO positive phases occur simultaneously ($\sim +4$ kW/m), creating a much-deepened Aleutian Low (Bonsal et al., 2001). These results are in line with previous studies that have analyzed the impact on wave parameters, separately, of the

PDO (Bromirski et al., 2013; Odériz, Silva, Mortlock, & Mendoza, et al., 2020) and of the ENSO (Izaguirre et al., 2011; Shimura et al., 2013; Stopa & Cheung, 2014; Yang & Oh, 2020).

Likewise, El Niño weakens the Walker cell and trade winds (Reiter, 1978), which aligns with a debilitated tropical WCT in the Indian Ocean (∼1 kW/m). Conversely, our investigation shows a reinforced tropical WCT in the Pacific during periods of El Niño. This may be associated with above-average tropical cyclone activity in the Pacific (Bell & Chelliah, 2006) during El Niño, and we should be cautious of taking only this averaged WCT for representing the region. On the other hand, the ENSO-negative phase weakens the Icelandic Low (Odériz, Silva, Mortlock, & Mori, 2020), and when is coupled with SAM a PDO, influences the dynamics of the polar WCT in the North Atlantic (∼7 kW/m).

A positive SAM increases the sea level pressure gradient between the extratropical and subtropical belts (Wang & Cai, 2013) and, as a result, intensifies the swells generated in the Southern Ocean (Godoi & Júnior, 2020). Consequently, a positive SAM also intensifies the ENSO wave power signal in the extratropical WCTs in the Indian Ocean (∼ + 6 kW/m) and the South Pacific (∼ + 6–9 kW/m). Waves and winds in the extratropical belt of the Southern Ocean have previously been identified as being highly affected by natural variation (Clem et al., 2020; Hemer et al., 2010; Wang & Cai, 2013). La Niña reinforces the wave power of the monsoon WCT in the Indian Ocean (∼ + 0.7 kW/m), due to the increase in the pressure gradient between the Indian Ocean and East Pacific (Wang et al., 2000; Wang & He, 2012; Zhang et al., 1996), a pattern which is reversed during El Niño. This effect is reinforced by the PDO (Wang et al., 2008), and when La Niña and a negative PDO coincide, the monsoon WCT strengthens (∼ + 0.8 kW/m). Positive SAM also amplifies the impact of La Niña on wave power for this WCT (∼ + 3 kW/m).

4. Historical Variability and Ocean Warming

The long-term trends in the spatially averaged wave direction (Dir_m), wave power (for both swell and wind seas combined, P_{wm}, and wind seas only, $P_{\mathrm{wm\text{-}ws}}$), and the occupied area (A_T) of each WCT were calculated over the same period as the natural variability analysis (1985–2018); see Figures 3(a-w), Figures 2a and Table S3. Only those trends that are significant to the 95% confidence level are discussed here.

Over the past 34 years, there has been a significant increase in wave power (∼3–9 kW/m) in both the extratropical and subtropical WCTs in the Southern Hemisphere, supporting the notion of an intensification of the wave climate in this Hemisphere, as suggested by other authors (Liu et al., 2016; Ribal & Young, 2019; Young et al., 2011). The increase in wave power in the Indian and South Atlantic Oceans coincides with a simultaneous increase in wind seas (+0.4 kW/m) and winds (+0.1–0.3 m/s). In addition, the region occupied by the subtropical WCT in the Indian Ocean has experienced a warming in SST of ∼0.6°C, over the same period.

Similarly, both wind speeds (∼0.2 m/s) and wave power (both for total swell and wind sea combined ∼2 kW/m and wind sea ∼0.4 kW/m) associated with the tropical WCTs in the Pacific and Atlantic Oceans have increased, as previously described by (England et al., 2014; Young & Ribal, 2019). The tropical regions of the Indian, Pacific, and Atlantic Oceans have all experienced warming of approximately 0.6°C. Similarly, the warm pool WCT shows a significant upward trend in wave power (∼1.6 kW/m), as do SSTs over the same area and time period (∼0.7°C). Here we find that the monsoon WCT shows a non-significant increase in wave power, although this trend is in agreement with other authors (Anoop et al., 2015), and this region also has the highest rate of SST warming (∼0.8°C). Conversely, it has been known for some time that wave power has reduced in the North Atlantic (Morim et al., 2019; Reguero et al., 2019), which we can now show is associated with the reduction in wave power of the subpolar WCT, although no links with SST warming and wind in this area were found. Results also indicate that in recent decades the area covered by this WCT has contracted.

Statistically significant trends in wave direction were only found for WCTs in the subtropical South Atlantic and polar North Atlantic. Neither of these changes appear to be related to SST warming, suggesting an alternative mechanism for shifts in wave direction. However, there is a general pattern of the high latitude WCTs (polar and extratropical) shifting poleward and the subtropical WCTs shifting toward the tropics. In

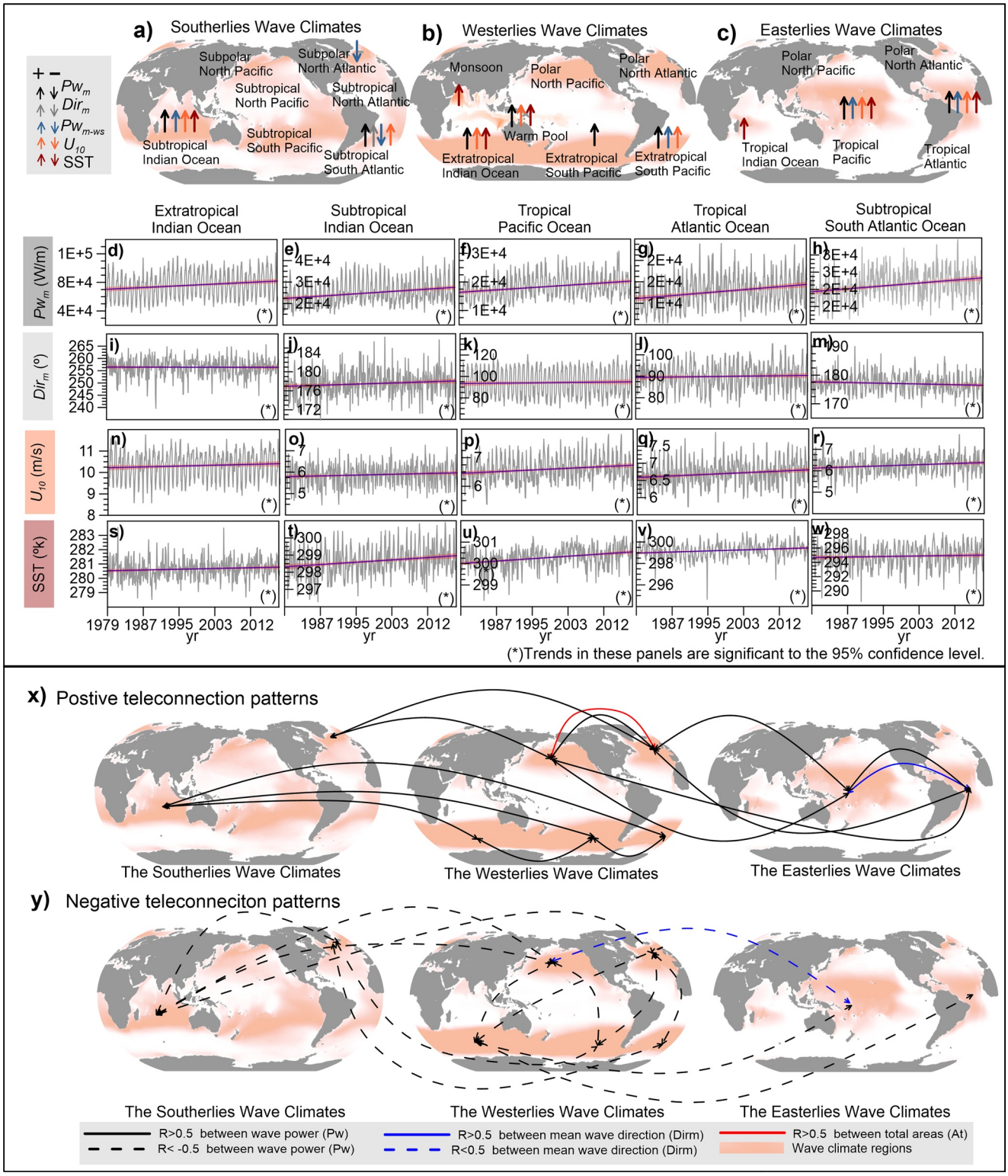

Figure 3. Trends of wave power (Pw_m), mean wave direction (Dir_m), wind-sea wave power ($Pw_{m\text{-}ws}$), wind velocity U_{10}, and sea surface temperature (SST) for (a) southerlies, (b) westerlies, and (c) easterlies wave climate types (WCTs). Time series and trends of WCTs (d)–(h) Pw_m (i–m) Dir_m (n–r) U_{10}, and (s–w) SST, for (d, i, n, s) the extratropical Indian Ocean (e, j, o, t) subtropical Indian Ocean (f, k, p, u) tropical Pacific (g, l, q, v) tropical Atlantic, and (h, m, r, w) subtropical South Atlantic. Correlation coefficients R for mean wave power, mean wave direction, and total area between the WCTs, x) positive correlation denoting either an increase/increase or decrease/decrease global teleconnection pattern, and y) negative correlation indicating an inverse (i.e., increase/decrease) teleconnection pattern.

the Southern Hemisphere, this is most probably related to a decrease in pressure across the high-latitudes (Clem et al., 2020).

In general, we found that the greatest changes in wave direction around the world are driven by natural variability. Overall, when summed across all WCTs, there is a net increase in global wave power, which is concentrated in the Southern Hemisphere. The global warming signal lies outside the upper bounds of natural variability in wave power for warm pool WCTs, the subtropical and the extratropical WCTs of the Indian Ocean, and the tropical WCTs of the Atlantic and Pacific basins. Extratropical WCTs in the South Pacific also show a significant upward trend in wave power that is greater than the anomalies produced by ENSO, although this appears not to be related to the global warming signal and is exceeded by variations induced by the ENSO and SAM when these climate patterns are coupled. A strong downward trend was found in wave power associated with the subpolar WCT in the North Atlantic but exceeded by natural variability when both negative ENSO and SAM phases occur. For other WCTs, including the subtropical South Pacific, the monsoon, the extratropical North Pacific, the tropical Indian Ocean and the Polar WCTs, the long-term trends over recent decades remain within the bounds of natural variability.

5. Ocean-Wave Teleconnection Patterns

Ocean-wave teleconnection patterns provide a basis for a global classification of coastal climates that link geographically disparate areas. The teleconnection patterns are distant wave climates having variability driven by remote climate forcing. The most well-known wave climate teleconnection is the relation between local wind sea and propagated swell (e.g., Delpey et al., 2010; Hanson & Phillips, 2001; Jiang, 2019). While the ocean-wave teleconnection patterns induced by remote regional winds is a topic not fully explored. The works of Echevarria et al. (2019) and Jiang (2020) analyzed seasonal variability at the global scale but do not examine the interconnected nature of hemispheric wave climate. The works of Semedo et al. (2011) and Stopa & Cheung (2014) examine wave climate teleconnections at the ocean basin scale. Reguero et al. (2019) explore global teleconnections between wave power and SST, but do not examine the causal mechanisms of these relationships via atmospheric pressure and surface wind patterns.

Results indicate that there are inter-basin, tropical-extratropical-subtropical, and inter-hemispheric connections between WCTs, not only related to their patterns of propagation but also by their origins in the atmospheric circulation. To analyze the interconnections between WCTs, the correlation coefficient (R) was calculated for wave power (P_{wm}) (Table S4), direction Dir_m (Table S5), and total area (A_T) for each WCT (Table S6).

For wave power, the results show a pan-hemispheric interconnection between WCTs that is influenced by seasonal variability, as shown in Figures 3x and 3y, commensurate with findings by other authors (Echevarria et al., 2019; Jiang, 2020). In the Southern Hemisphere, the extratropical and subtropical WCTs exhibit the same response to atmospheric variability. However, in the Atlantic and Pacific basins, the tropical WCTs intensify simultaneously with the extratropical and subtropical WCTs of the Northern Hemisphere (see Figure 1 and Figure S6-S7). This concurrent behavior indicates that these WCTs are all governed by the intensity and position of the Northern Hemisphere subtropical high-pressure belt.

For wave direction, it was found that the subtropical WCT in the Indian Ocean rotates in the opposite direction to the extratropical WCTs in the Pacific and Indian Ocean. All extratropical WCTs rotate in the same direction, with the exception of that in the North Atlantic basin that is dominated by the position and intensity of the Icelandic Low. The tropical WCTs in the Pacific and Atlantic all rotate in line with movements in the Hadley cells.

Through this mechanism, we can identify coasts where Extratropical WCTs prevail, such as those of Chile, the Mexican Pacific, Northwest Europe, Southern Africa and South Australia, and those where tropical WCTs dominate, including those bounding the Caribbean Sea, Indonesia, Madagascar or East of Australia. Other regions are intermittently dominated by both tropical and subtropical WCTs (e.g., the coasts of Japan and Argentina, Eastern New Zealand, and Eastern USA). These regions have the same wave conditions throughout the year (Fairley et al., 2020).

6. Conclusions

A novel "dynamic clustering" method was developed to classify the global ocean WCTs according to the planetary wind systems responsible for their genesis, allowing them to be traceable in time and space across the world's oceans. At the highest-level, the global ocean wave climate is classified into the extratropical, monsoon, warm pool, subtropical, subpolar, polar, and tropical WCTs.

Results suggest that natural variability is the principal driver of variations in the subtropical WCT of the South Pacific Ocean, the monsoon, the extratropical WCTs of the Pacific, the tropical WCT of the Indian Ocean, and the Polar WCTs, over the last 34 years. The WCTs in which changes in wave conditions are linked to a global warming signal include the warm pool, extratropical, and subtropical WCTs of the Indian Ocean, and the tropical WCTs of the Atlantic and Pacific Oceans. WCTs with large natural variability may mask a global warming signal that is emerging, but, because of large internal fluctuations, this signal takes longer to emerge than in regions with less variation. Although we could not identify the driver, a strong long-term trend was detected in the extratropical WCT of the South Pacific (~6 kW/m) but this was masked by natural variability when the positive phases of ENSO and SAM occurred simultaneously (up to 10 kW/m). In the next century, the ENSO (Cai et al., 2015) and SAM (Arblaster & Meehl, 2006) are projected to intensify, and Global Couple Models have limitations in capturing both when coupled (Lim et al., 2016). This study can diminish the uncertainty of their impacts in projected wave climate and provide relevant information on quantifying the natural variability and global warming for coastal hazard assessments.

In addition, global wave climate teleconnection patterns were explored. The WCTs exhibit strong inter-basin, inter-hemisphere, and tropical-subtropical-extratropical-subpolar teleconnections in different regions of the world. This implies a level of connection between coastal areas where the same WCTs prevail, driven by remote wind systems. A coastal management framework built on wave climate types-dominated coasts could deliver key opportunities for climate change adaptation and mitigation on national and pan-national levels. Likewise, to identify the transitional wave climate regions (e.g., tropical-subtropical) (Duarte et al., 2020; Wernberg et al., 2016). These transition zones are those most likely to experience a shift in the prevailing climate, giving rise to wave conditions that exceed the thresholds of the current natural variability. As such, further research into the vulnerability of these locations to wave climate changes is needed.

Data Availability Statement

Wave and wind data is from the European Center for Medium-Range Weather Forecasts (https://www.ecmwf.int/en/forecasts/datasets/reanalysis-datasets/era5). The climate index is from NOAA (https://psl.noaa.gov/data/climateindices/list/). The SST data is from Climate Forecast System Reanalysis (https://www.ncdc.noaa.gov/data-access/model-data/model-datasets/climate-forecast-system-version2-cfsv2). A repository data is provided in: http://dx.doi.org/10.17632/mh9d3494kp.1

Acknowledgments
This work was financed by Fondo CONACYT-SENER/Sustentabilidad Energética through the Centro Mexicano de Inovación en Energías del Océano (CEMIE-Océano), grant number 249795; and DPRI research funds, JSPS KAKENHI and Integrated Research Program for Advancing Climate Models (TOUGOU Program: JPMXD0717935498) supported by MEXT of Japan. The authors want to thank David K. Adams and Stipo Sentic for discussions at the initial stages of this research.

References

Alves, J.-H. G. M. (2006). Numerical modeling of ocean swell contributions to the global wind-wave climate. *Ocean Modelling*, *11*(1), 98–122 https://doi.org/10.1016/j.ocemod.2004.11.007

Anoop, T. R., Kumar, V. S., Shanas, P. R., & Johnson, G. (2015). Surface wave climatology and its variability in the North Indian Ocean based on ERA-Interim reanalysis. *Journal of Atmospheric and Oceanic Technology*, *32*(7), 1372–1385. https://doi.org/10.1175/JTECH-D-14-00212.1

Arblaster, J. M., & Meehl, G. A. (2006). Contributions of external forcings to southern annular mode trends. *Journal of Climate*, *19*(12), 2896–2905. https://doi.org/10.1175/JCLI3774.1

Barnard, P. L., Short, A. D., Harley, M. D., Splinter, K. D., Vitousek, S., Turner, I. L., et al. (2015). Coastal vulnerability across the Pacific dominated by El Niño/Southern Oscillation. *Nature Geoscience*, *8*, 801–807. https://doi.org/10.1038/ngeo2539

Bell, G. D., & Chelliah, M. (2006). Leading tropical modes associated with interannual and multidecadal fluctuations in North Atlantic hurricane activity. *Journal of Climate*, *19*(4), 590–612. https://doi.org/10.1175/JCLI3659.1

Bonsal, B. R., Shabbar, A., & Higuchi, K. (2001). Impacts of low frequency variability modes on Canadian winter temperature. *International Journal of Climatology*, *21*(1), 95–108. https://doi.org/10.1002/joc.590

Bromirski, P. D., Cayan, D. R., Helly, J., & Wittmann, P. (2013). Wave power variability and trends across the North Pacific. *J. Geophys. Res. Oceans*, *118*(12), 6329–6348. https://doi.org/10.1002/2013JC009189

Cai, W., Santoso, A., Wang, G., Yeh, S.-W., An, S.-I., Cobb, K. M., et al. (2015). ENSO and greenhouse warming. *Nature Climate Change*, *5*(9), 849–859. https://doi.org/10.1038/nclimate2743

Clem, K. R., Fogt, R. L., Turner, J., Lintner, B. R., Marshall, G. J., Miller, J. R., & Renwick, J. A. (2020). Record warming at the South Pole during the past three decades. *Nature Climate Change*, *10*(8), 762–770. https://doi.org/10.1038/s41558-020-0815-z

Delpey, M. T., Ardhuin, F., Collard, F., & Chapron, B. (2010). Space-time structure of long ocean swell fields. *Journal of Geophysical Research*, *115*, C12037. https://doi.org/10.1029/2009JC005885

Deser, C., Knutti, R., Solomon, S., & Phillips, A. S. (2012). Communication of the role of natural variability in future North American climate. *Nature Climate Change*, *2*(11), 775–779. https://doi.org/10.1038/nclimate1562

Duarte, C. M., Agusti, S., Barbier, E., Britten, G. L., Castilla, J. C., Gattuso, J.-P., et al. (2020). Rebuilding marine life. *Nature*, *580*(7801), 39–51. https://doi.org/10.1038/s41586-020-2146-7

Echevarria, E. R., Hemer, M. A., & Holbrook, N. J. (2019). Seasonal variability of the global spectral wind wave climate. *J. Geophys. Res. Oceans*, *124*(4), 2924–2939. https://doi.org/10.1029/2018JC014620

Echevarria, E. R., Hemer, M. A., Holbrook, N. J., & Marshall, A. G. (2020). Influence of the Pacific-South American modes on the global spectral wind-wave climate. *J. Geophys. Res. Oceans*, *125*(8), e2020JC016354. https://doi.org/10.1029/2020JC016354

England, M. H., McGregor, S., Spence, P., Meehl, G. A., Timmermann, A., Cai, W., et al. (2014). Recent intensification of wind-driven circulation in the Pacific and the ongoing warming hiatus. *Nature Climate Change*, *4*(3), 222–227. https://doi.org/10.1038/nclimate2106

Erftemeijer, P. L. A., Riegl, B., Hoeksema, B. W., & Todd, P. A. (2012). Environmental impacts of dredging and other sediment disturbances on corals: A review. *Marine Pollution Bulletin*, *64*(9), 1737–1765. https://doi.org/10.1016/j.marpolbul.2012.05.008

Fairley, I., Lewis, M., Robertson, B., Hemer, M., Masters, I., Horrillo-Caraballo, J., et al. (2020). A classification system for global wave energy resources based on multivariate clustering. *Applied Energy*, *262*, 114515. https://doi.org/10.1016/j.apenergy.2020.114515

Fraser, C. I., Morrison, A. K., Hogg, A. M., Macaya, E. C., van Sebille, E., Ryan, P. G., et al. (2018). Antarctica's ecological isolation will be broken by storm-driven dispersal and warming. *Nature Climate Change*, *8*(8), 704–708. https://doi.org/10.1038/s41558-018-0209-7

Godoi, V. A., & Torres Júnior, A. R. (2020). A global analysis of austral summer ocean wave variability during SAM-ENSO phase combinations. *Climate Dynamics*, *54*(9), 3991–4004. https://doi.org/10.1007/s00382-020-05217-2

Godwyn-Paulson, P., Jonathan, M. P., Hernandez, F. R., Muthusankar, G., & Lakshumanan, C. (2020). Coastline variability of several Latin American cities alongside Pacific Ocean due to the unusual "Sea Swell" events of 2015. *Environmental Monitoring and Assessment*, *192*(8), 522. https://doi.org/10.1007/s10661-020-08469-x

Hanson, J. L., & Phillips, O. M. (2001). Automated analysis of ocean surface directional wave spectra. *Journal of Atmospheric and Oceanic Technology*, *18*, 277–293. https://doi.org/10.1175/1520-0426(2001)018<0277:aaoosd>2.0.co;2

Hemer, M. A., Church, J. A., & Hunter, J. R. (2010). Variability and trends in the directional wave climate of the Southern Hemisphere. *International Journal of Climatology*, *30*(4), 475–491. https://doi.org/10.1002/joc.1900

Hemer, M. A., Fan, Y., Mori, N., Semedo, A., & Wang, X. L. (2013). Projected changes in wave climate from a multi-model ensemble. *Nature Climate Change*, *3*(5), 471–476. https://doi.org/10.1038/nclimate1791

Hemer, M. A., Katzfey, J., & Trenham, C. E. (2013). Global dynamical projections of surface ocean wave climate for a future high greenhouse gas emission scenario. *Ocean Modelling*, *70*, 221–245. https://doi.org/10.1016/j.ocemod.2012.09.008

Hersbach, H., Bell, B., Berrisford, P., Hirahara, S., Horányi, A., Muñoz-Sabater, J., et al. (2020). The ERA5 global reanalysis. *Quarterly Journal of the Royal Meteorological Society*, *146*(730), 1999–2049. https://doi.org/10.1002/qj.3803

Hirsch, R. M., Slack, J. R., & Smith, R. A. (1982). Techniques of trend analysis for monthly water quality data. *Water Resources Research*, *18*(1), 107–121. https://doi.org/10.1029/WR018i001p00107

Huizer, S., Luijendijk, A. P., Bierkens, M. F. P., & Oude Essink, G. H. P. (2019). Global potential for the growth of fresh groundwater resources with large beach nourishments. *Scientific Reports*, *9*(1), 12451. https://doi.org/10.1038/s41598-019-48382-z

Izaguirre, C., Losada, I. J., Camus, P., Vigh, J. L., & Stenek, V. (2020). Climate change risk to global port operations. *Nature Climate Change*, *11*, 14–20. https://doi.org/10.1038/s41558-020-00937-z

Izaguirre, C., Méndez, F. J., Menéndez, M., & Losada, I. J. (2011). Global extreme wave height variability based on satellite data. *Geophysical Research Letters*, *38*(10), L10607. https://doi.org/10.1029/2011GL047302

Jiang, H. (2019). Spatially tracking wave events in partitioned numerical wave model outputs. *Journal of Atmospheric and Oceanic Technology*, *36*(10), 1933–1944. https://doi.org/10.1175/JTECH-D-18-0228.1

Jiang, H. (2020). Wave climate patterns from spatial tracking of global long-term ocean wave spectra. *Journal of Climate*, *33*(8), 3381–3393. https://doi.org/10.1175/JCLI-D-19-0729.1

Kendall, M. G. (1948). *Rank correlation methods. Rank correlation methods*. Griffin.

Ketchen, D. J., & Shook, C. L. (1996). The application of cluster analysis in strategic management research: An analysis and critique. *Strategic Management Journal*, *17*(6), 441–458. https://doi.org/10.1002/(SICI)1097-0266(199606)17:6<441::AID-SMJ819>3.0.CO;2-G

Kirezci, E., Young, I. R., Ranasinghe, R., Muis, S., Nicholls, R. J., Lincke, D., & Hinkel, J. (2020). Projections of global-scale extreme sea levels and resulting episodic coastal flooding over the 21st Century. *Scientific Reports*, *10*(1), 11629. https://doi.org/10.1038/s41598-020-67736-6

Li, F., Wang, H., & Gao, Y. (2015). Modulation of Aleutian low and Antarctic oscillation co-variability by ENSO. *Climate Dynamics*, *44*(5), 1245–1256. https://doi.org/10.1007/s00382-014-2134-4

Lim, E.-P., Hendon, H. H., Arblaster, J. M., Delage, F., Nguyen, H., Min, S.-K., & Wheeler, M. C. (2016). The impact of the southern annular mode on future changes in southern hemisphere rainfall. *Geophysical Research Letters*, *43*(13), 7160–7167. https://doi.org/10.1002/2016GL069453

Liu, Q., Babanin, A. V., Zieger, S., Young, I. R., & Guan, C. (2016). Wind and wave climate in the Arctic Ocean as observed by altimeters. *Journal of Climate*, *29*(22), 7957–7975. https://doi.org/10.1175/JCLI-D-16-0219.1

Li, X. M. (2016). A new insight from space into swell propagation and crossing in the global oceans. *Geophysical Research Letters*, *43*(10), 5202–5209. https://doi.org/10.1002/2016GL068702

Lobeto, H., Menendez, M., & Losada, I. J. (2021). Future behavior of wind wave extremes due to climate change. *Scientific Reports*, *11*(1), 7869. https://doi.org/10.1038/s41598-021-86524-4

Luijendijk, A., Hagenaars, G., Ranasinghe, R., Baart, F., Donchyts, G., & Aarninkhof, S. (2018). The state of the world's beaches. *Scientific Reports*, *8*(1), 6641. https://doi.org/10.1038/s41598-018-24630-6

MacQueen, J. (1967). Some methods for classification and analysis of multivariate observations. Proceedings of the Fifth Berkeley Symposium on Mathematical Statistics and Probability (Vol. 1, 281–297). StatisticsUniversity of California Press. Retrieved from https://projecteuclid.org/euclid.bsmsp/1200512992

Marshall, A. G., Hemer, M. A., Hendon, H. H., & McInnes, K. L. (2018). Southern annular mode impacts on global ocean surface waves. *Ocean Modelling*, *129*, 58–74. https://doi.org/10.1016/j.ocemod.2018.07.007

Melet, A., Meyssignac, B., Almar, R., & Le Cozannet, G. (2018). Under-estimated wave contribution to coastal sea-level rise. *Nature Climate Change*, *8*(3), 234–239. https://doi.org/10.1038/s41558-018-0088-y

Meucci, A., Young, I. R., Hemer, M., Kirezci, E., & Ranasinghe, R. (2020). Projected 21st century changes in extreme wind-wave events. *Science Advances*, *6*(24), eaaz7295. https://doi.org/10.1126/sciadv.aaz7295

Morim, J., Hemer, M., Wang, X. L., Cartwright, N., Trenham, C., Semedo, A., et al. (2019). Robustness and uncertainties in global multivariate wind-wave climate projections. *Nature Climate Change*, *9*(9), 711–718. https://doi.org/10.1038/s41558-019-0542-5

Moser, S. C., & Ekstrom, J. A. (2010). A framework to diagnose barriers to climate change adaptation. *Proceedings of the National Academy of Sciences of the United States of America*, *107*(51), 22026–22031. https://doi.org/10.1073/pnas.1007887107

Newman, M., Compo, G. P., & Alexander, M. A. (2003). ENSO-Forced variability of the Pacific decadal oscillation. *Journal of Climate*, *16*(23), 3853–3857. https://doi.org/10.1175/1520-0442(2003)016<3853:EVOTPD>2.0.CO;2

Odériz, I., Gómez, I., Ventura, Y., Díaz, V., Escalante, A., Gómez, D. T., et al., (2020). Understanding drivers of connectivity and resilience under tropical cyclones in coastal ecosystems at Puerto Morelos, Mexico. *Journal of Coastal Research*, *95*(sp1), 128–132. https://doi.org/10.2112/SI95-025.1

Odériz, I., Silva, R., Mortlock, T. R., & Mendoza, E. (2020). Climate drivers of directional wave power on the Mexican coast. *Ocean Dynamics*, *70*(9), 1253–1265. https://doi.org/10.1007/s10236-020-01387-z

Odériz, I, Silva, R, Mortlock, T. R, & Mori, N (2020). El Niño-Southern oscillation impacts on global wave climate and potential coastal hazards. *Journal of Geophysical Research Oceans*, *125*, e2020JC016464. https://doi.org/10.1029/2020JC016464

Ranasinghe, R. (2016). Assessing climate change impacts on open sandy coasts: A review. *Earth-Science Reviews*, *160*, 320–332. https://doi.org/10.1016/j.earscirev.2016.07.011

Reguero, B. G., Losada, I. J., & Méndez, F. J. (2015). A global wave power resource and its seasonal, interannual and long-term variability. *Applied Energy*, *148*, 366–380. https://doi.org/10.1016/j.apenergy.2015.03.114

Reguero, B. G., Losada, I. J., & Méndez, F. J. (2019). A recent increase in global wave power as a consequence of oceanic warming. *Nature Communications*, *10*(1), 1–14. https://doi.org/10.1038/s41467-018-08066-0

Reiter, E. R. (1978). The interannual variability of the ocean-atmosphere system. *Journal of the Atmospheric Sciences*, *35*(3), 349–370. https://doi.org/10.1175/1520-0469(1978)035<0349:TIVOTO>2.0.CO;2

Ribal, A., & Young, I. R. (2019). 33 years of globally calibrated wave height and wind speed data based on altimeter observations. *Scientific Data*, *6*(1), 77. https://doi.org/10.1038/s41597-019-0083-9

Semedo, A., Sušelj, K., Rutgersson, A., & Sterl, A. (2011). A global view on the wind sea and swell climate and variability from ERA-40. *Journal of Climate*, *24*(5), 1461–1479. https://doi.org/10.1175/2010JCLI3718.1

Shimura, T., Hemer, M., Lenton, A., Chamberlain, M. A., & Monselesan, D. (2020). Impacts of ocean wave-dependent momentum flux on global ocean climate. *Geophysical Research Letters*, *47*(20), e2020GL089296. https://doi.org/10.1029/2020GL089296

Shimura, T., Mori, N., & Mase, H. (2013). Ocean waves and teleconnection patterns in the northern hemisphere. *Journal of Climate*, *26*(21), 8654–8670. https://doi.org/10.1175/JCLI-D-12-00397.1

Stopa, J. E., & Cheung, K. F. (2014). Periodicity and patterns of ocean wind and wave climate. *Journal of Geophysical Research: Oceans*, *119*(8), 5563–5584. https://doi.org/10.1002/2013JC009729

Tebaldi, C., Arblaster, J. M., & Knutti, R. (2011). Mapping model agreement on future climate projections. *Geophysical Research Letters*, *38*(23, a, n). https://doi.org/10.1029/2011GL049863

Toimil, A., Camus, P., Losada, I. J., Le Cozannet, G., Nicholls, R. J., Idier, D., & Maspataud, A. (2020). Climate change-driven coastal erosion modeling in temperate sandy beaches: Methods and uncertainty treatment. *Earth-Science Reviews*, *202*, 103110. https://doi.org/10.1016/j.earscirev.2020.103110

Wang, B., Wu, R., & Fu, X. (2000). Pacific-East Asian teleconnection: How does ENSO affect East Asian Climate? *Journal of Climate*, *13*(9), 1517–1536. https://doi.org/10.1175/1520-0442(2000)013<1517:PEATHD>2.0.CO;2

Wang, G., & Cai, W. (2013). Climate-change impact on the 20th-century relationship between the southern annular mode and global mean temperature. *Scientific Reports*, *3*(1), 2039. https://doi.org/10.1038/srep02039

Wang, H., & He, S. (2012). Weakening relationship between East Asian winter monsoon and ENSO after mid-1970s. *Chinese Science Bulletin*, *57*(27), 3535–3540. https://doi.org/10.1007/s11434-012-5285-x

Wang, L., Chen, W., & Huang, R. (2008). Interdecadal modulation of PDO on the impact of ENSO on the east Asian winter monsoon. *Geophysical Research Letters*, *35*(20). L20702. https://doi.org/10.1029/2008GL035287

Wernberg, T., Bennett, S., Babcock, R. C., de Bettignies, T., Cure, K., Depczynski, M., et al. (2016). Climate-driven regime shift of a temperate marine ecosystem. *Science*, *353*(6295), 169–172. https://doi.org/10.1126/science.aad8745.LP – 172

Yang, S., & Oh, J.-H. (2020). Effects of modes of climate variability on wave power during boreal summer in the western North Pacific. *Scientific Reports*, *10*(1), 5187. https://doi.org/10.1038/s41598-020-62138-0

Young, I. R., & Ribal, A. (2019). Multiplatform evaluation of global trends in wind speed and wave height. *Science*, *364*(6440), 548–552. https://doi.org/10.1126/science.aav9527.LP – 552

Young, I. R., Zieger, S., & Babanin, A. V. (2011). Global trends in wind speed and wave height. *Science*, *332*, 451–456. https://doi.org/10.1126/science.1197219

Young, I. R., Zieger, S., & Babanin, A. V. (2011). Global trends in wind speed and wave height. *Science*, *332*(6028), 451–455. https://doi.org/10.1126/science.1197219

Zhang, R, Sumi, A, & Kimoto, M (1996). Impact of El Niño on the East Asian Monsoon. *Journal of the Meteorological Society of Japan*, *74*(1), 49–62. https://doi.org/10.2151/jmsj1965.74.1_49

References From the Supporting Information

Berkhin, P. (2006). *A survey of clustering data mining techniques BT - grouping multidimensional data: Recent advances in clustering*. In J. Kogan, C. Nicholas, & M. Teboulle, (Eds.), (25–71). Springer Berlin Heidelberg. https://doi.org/10.1007/3-540-28349-8_2

Broccoli, A. J., Dahl, K. A., & Stouffer, R. J. (2006). Response of the ITCZ to Northern Hemisphere cooling. *Geophysical Research Letters*, *33*(1), 1–4. https://doi.org/10.1029/2005GL024546

Dodet, G., Bertin, X., & Taborda, R. (2010). Wave climate variability in the North-East Atlantic Ocean over the last six decades. *Ocean Modelling*, *31*(3–4), 120–131. https://doi.org/10.1016/j.ocemod.2009.10.010

Guenther, H., Hasselmann, S., & Janssen, P. A. E. M. (1992). *The WAM model cycle 4. Germany*. Retrieved from http://inis.iaea.org/search/search.aspx?orig_q=RN:26000788

Pickart, R. S., Macdonald, A. M., Moore, G. W. K., Renfrew, I. A., Walsh, J. E., & Kessler, W. S. (2009). Seasonal evolution of Aleutian low pressure systems: Implications for the North Pacific Subpolar circulation. *Journal of Physical Oceanography*, *39*(6), 1317–1339. https://doi.org/10.1175/2008JPO3891.1

Saha, S., Moorthi, S., Pan, H.-L., Wu, X., Wang, J., Nadiga, S., et al. (2010). *NCEP climate Forecast system Reanalysis (CFSR) selected hourly time-series products, January 1979 to December 2010*. Research Data Archive at the National Center for Atmospheric Research, Computational and Information Systems Laboratory. https://doi.org/10.5065/D6513W89

Saha, S., Moorthi, S., Wu, X., Wang, J., Nadiga, S., Tripp, P., et al. (2011). *NCEP climate Forecast system Version 2 (CFSv2) 6-hourly products*. Research Data Archive at the National Center for Atmospheric Research, Computational and Information Systems Laboratory. https://doi.org/10.5065/D61C1TXF

Sanil Kumar, V., Johnson, G., Udhaba, D. G., Chempalayil, S. P., Singh, J. A. I., & Pednekar, P. (2012). Variations in nearshore waves along Karnataka, west coast of India. *Journal of Earth System Science*, *121*(2), 393–403. https://doi.org/10.1007/s12040-012-0160-3

Shimura, T., & Mori, N. (2019). High-resolution wave climate hindcast around Japan and its spectral representation. *Coastal Engineering*, *151*, 1–9. https://doi.org/10.1016/j.coastaleng.2019.04.013

Webb, A., & Fox-Kemper, B. (2011). Wave spectral moments and Stokes drift estimation. *Ocean Modelling*, *40*(3), 273–288. https://doi.org/10.1016/j.ocemod.2011.08.007